

TM - 82969
(replacement copy)

NASA Technical Memorandum 82969

NASA-TM-82969 19830004087

Turbulent Solution of the Navier-Stokes Equations for an Inhomogeneous Developing Shear Layer

(NASA-TM-82969) TURBULENT SOLUTION OF THE NAVIER-STOKES EQUATIONS FOR AN INHOMOGENEOUS DEVELOPING SHEAR LAYER (NASA) 14 p HC A02/MF A01

R83-12357

CSSL 20D 63
82/34

Unclas
01115

R. G. Deissler
Lewis Research Center
Cleveland, Ohio



Prepared for the
American Physical Society Meeting on Fluid Dynamics
New Brunswick, New Jersey, November 21-23, 1982

NASA



NF00335

MAY 2 2000



Turbulent solution of the Navier-Stokes equations for
an inhomogeneous developing shear layer

R. G. Deissler

National Aeronautics and Space Administration
Lewis Research Center
Cleveland, Ohio 44135

ABSTRACT

To study the nonlinear physics of inhomogeneous turbulent shear flow, the unaveraged Navier-Stokes equations are solved numerically. For initial conditions a three-dimensional cosine velocity fluctuation and a mean-velocity profile with a step are used. Although the initial conditions are nonrandom, the flow soon becomes turbulent. Concentrated turbulent energy develops near the plane where the mean velocity gradient is initially infinite. The terms in the one-point correlation equation for turbulent energy, including those for the diffusion and production of turbulence, are calculated; the diffusion terms tend to make the turbulence more homogeneous.

The production, transfer between eddy sizes, and dissipation of turbulent energy have been studied numerically.^{1,2} In those references the turbulence is homogeneous, and no net spatial diffusion occurs.

Here, the work is extended to an inhomogeneous developing shear layer so that diffusion, as well as the other turbulence processes, can be considered. The initial condition chosen for this purpose is, in dimensionless form

$$\tilde{u}_i = \sum_{n=1}^3 a_i^n \cos \vec{q}^n \cdot \vec{x} + \pi \delta_{i1} V [\text{sgn}(x_2 - \pi) + 1] \quad (1)$$

where

$$\tilde{u}_i = \frac{x_0}{v} \tilde{u}_i^*, \quad V = \frac{x_0}{v} V^*, \quad a_i^n = \frac{x_0}{v} a_i^{*n}, \quad \text{and} \quad x_i = \frac{x_i^*}{x_0}.$$

Note that the stars on dimensional quantities are omitted for corresponding dimensionless quantities. The subscripts can assume the values 1, 2, and 3. The quantity \tilde{u}_i^* is an instantaneous velocity component, V^* is a constant with the dimensions of a velocity, a_i^{*n} is an initial velocity amplitude or Fourier component of the disturbance, \vec{q}^{*n} is an initial wavenumber vector, x_i^* is a space coordinate, x_0 is an initial characteristic length, v is the kinematic viscosity, δ_{ij} is the Kronecker delta (equals 1 for $i = j$ and 0 for $i \neq j$), and $\text{sgn } x$ designates the sign of x . The quantities $\vec{q}^n \cdot \vec{x}$ are dot products. The first term on the right side of Eq. (1) is the fluctuating part of the initial \tilde{u}_i , and the second term is the initial mean velocity. The latter is plotted against x_2 in the curve for $t = 0$ in Fig. 1. In order to satisfy the continuity condition

$$\frac{\partial \tilde{u}_i}{\partial x_i} = 0 \quad (2)$$

$$a_i^n q_i^n = 0 \quad (3)$$

For the present work

$$a_i^1 = k(2, -1, 1), \quad a_i^2 = k(1, -2, 1), \quad a_i^3 = k(1, -1, 2)$$

and

$$q_i^1 = (-1, -1, 1), \quad q_i^2 = (1, 1, 1), \quad q_i^3 = (1, -1, -1), \quad (4)$$

where k is a quantity that fixes the Reynolds number. In addition to satisfying continuity, Eq. (4) gives

$$\overline{u_1^2} = \overline{u_2^2} = \overline{u_3^2} = \overline{u_0^2} \quad (5)$$

at the initial time, where $u_i = \tilde{u}_i - \delta_{i1} U_1$, U_i is a mean velocity component and the overbars indicate averaged values. Thus, Eqs. (1) and (4) give a particularly simple initial condition, as the components of the mean-square velocity fluctuation are initially equal.

The components in Eqs. (4) are the same as those in the earlier works^{1,2} except that the signs of the a_2^n and q_2^n have been changed to make the initial $\overline{u_1 u_2}$ negative. Thus, $\overline{u_1 u_2}$ does not have to change sign as a result of the dynamics of the flow, as it did in the earlier work, and the initial adjustment period is eliminated. If the adjustment period remained, much of the development of the shear layer would be distorted.

To calculate the evolution of \tilde{u}_i , the Navier-Stokes equations can be written in dimensionless form as

$$\frac{\partial \tilde{u}_i}{\partial t} = - \frac{\partial (\tilde{u}_i \tilde{u}_k)}{\partial x_k} - \frac{\partial \tilde{p}}{\partial x_i} + \frac{\partial^2 \tilde{u}_i}{\partial x_k \partial x_k} \quad (6)$$

where \tilde{p} is given by the Poisson equation

$$\frac{\partial^2 \tilde{p}}{\partial x_\ell \partial x_\ell} = \frac{\partial^2 (\tilde{u}_\ell \tilde{u}_k)}{\partial x_\ell \partial x_k}, \quad (7)$$

$$t = \frac{v}{x_0} t^*, \text{ and } \tilde{p} = \frac{x_0^2}{\rho v^2} \tilde{p}^* .$$

The quantity t^* is the time, p^* is the pressure, and ρ is the density; the rest of the symbols are defined after Eq. (1). A repeated subscript in a term indicates a summation of terms. Equation (7) is obtained by taking the divergence of Eq. (6) and using the continuity equation, Eq. (2).

In order to carry out the numerical solution of Eqs. (6) and (7) subject to the initial conditions of Eqs. (1) and (4), a cubical grid with 32^3 points and with faces at $x_i = 0$ and 2π is used. Modified periodicity is assumed for boundary conditions;¹ that is,

$$(\tilde{u}_i)_{x_j=2\pi+b_j} = (\tilde{u}_i)_{x_j=b_j} + 2\pi \delta_{i1} \delta_{j2} V \quad (8)$$

and

$$(\tilde{p})_{x_j=2\pi+b_j} = (\tilde{p})_{x_j=b_j} \quad (9)$$

for any b_j . Equation (8) (not a tensor equation) is consistent with the initial condition given by Eq. (1) and is used to numerically calculate derivatives at the boundaries.

The spatial- and time-differencing schemes are essentially those used by Clark, et al.³ and in Refs. 1 and 2; that is, for the spatial derivatives, centered fourth-order difference expressions are used. For time-differencing a predictor-corrector method with a second-order predictor and a third-order corrector is used. The Poisson equation for the pressure is solved directly by a fast Fourier-transform method, which preserves continuity quite well.

The calculated evolution of the mean velocity U_1 (U_2 and U_3 are zero) is plotted against x_2 in Fig. 1. The mean velocity is obtained by averaging u_1 over x_1 and x_3 at fixed values of x_2 . The shear layer grows (from essentially zero initial thickness) because of the presence of the turbulent and viscous shear stresses. The ratio of turbulent to viscous shear stress (averaged over x_1 and x_3 at the central plane $x_2 = \pi$) is plotted against dimensionless time in Fig. 2. Except at very early times the growth of the shear layer is almost completely dominated by the turbulent shear stress.

Figure 3 shows the evolution of the instantaneous velocity component u_2 and of the root-mean-square value of u_2 (averaged over the central plane $x_2 = \pi$). Although the initial conditions are nonrandom, the evolution of u_2 has a random appearance. On the other hand $\overline{u_2^2}^{1/2}$ evolves smoothly. These characteristics are representative of a turbulent flow. The quantity $\overline{u_2^2}^{1/2}$ increases monotonically at small times in contrast to the corresponding curve in Ref. 1, where an initial adjustment period was present. As mentioned earlier (after Eqs. (4)), the initial adjustment period has been eliminated here by changing the sign of the initial u_2 , so that $\overline{u_1 u_2}$ does not have to change sign as a result of the dynamics of the turbulence. The

decrease in $\overline{u_2^2}^{1/2}$ near the end of the curve is caused by a decrease in mean velocity gradient, and thus of turbulence production, at large times (Fig. 1).

As in the homogeneous case¹, small-scale fluctuations are generated in the inhomogeneous turbulence in Fig. 3 by the interaction of the mean velocity with the turbulence. This can be seen by comparison of Fig. 3 with Fig. 1(a) in Refs. 1 and 2, where mean velocity gradients are absent. One might expect this, since it has been shown⁴ that even for a general inhomogeneous turbulence, a term in the two-point spectral equation for the turbulence can transfer energy between scales of motion as a result of the presence of mean gradients.

A dimensionless plot of turbulent kinetic energy as a function of x_2 and time is given in Fig. 4. As for all of the averaged values, $\overline{u_k u_k}/2$ is averaged over x_1 and x_3 for fixed values of x_2 . As time increases, an intense concentration of turbulent energy develops near the plane $x_2 = \pi$, where the mean velocity gradient is initially infinite. The turbulence is highly inhomogeneous. Inhomogeneity, in fact, seems to be the dominant characteristic of the turbulence generated in the shear layer. The indicated increase of turbulence with time is similar to that obtained experimentally.⁵

Terms in the one-point correlation equation for the rate of change of the turbulent kinetic energy

$$\frac{\partial}{\partial t} \left(\frac{\overline{u_k u_k}}{2} \right) = - \overline{u_1 u_2} \frac{dU_1}{dx_2} - \frac{\partial}{\partial x_2} \overline{p u_2} - \frac{\partial}{\partial x_2} \left(\frac{\overline{u_k u_k}}{2} u_2 \right) - \frac{\partial^2}{\partial x_2^2} \left(\frac{\overline{u_k u_k}}{2} \right) - \frac{\partial u_k}{\partial k_l} \frac{\partial u_k}{\partial x_l} \quad (10)$$

are plotted for $t = 0.000293$ in Fig. 5. Equation (10) is constructed from Eq. (6) after letting $\tilde{u}_i = u_i + U_i$ and $\tilde{p} = p + P$. The terms that contribute most to the rate of change of $\overline{u_k u_k}/2$ are the production term

$-\overline{u_1 u_2} \, dU_1/dx_2$, the pressure diffusion term $-\overline{\partial p u_2}/\partial x_2$ and the kinetic-energy diffusion term $-(1/2)\partial \overline{u_k u_k u_2}/\partial x_2$. The viscous diffusion term $-\partial^2(\overline{u_k u_k}/2)/\partial x_2^2$ and the dissipation term $-\overline{\partial u_k/\partial x_k \partial u_k/\partial x_k}$ are small in Fig. 5. At early times, however, when the mean velocity gradient is large, the dissipation term is appreciable.

The production term, whose form shows that turbulent energy is produced by work done on the Reynolds shear stress by the mean velocity gradient, is largest near the plane $x_2 = \pi$, where the velocity gradient is initially infinite. The plots of the pressure and kinetic-energy diffusion terms show that those terms are negative near $x_2 = \pi$ and positive away from that plane. Thus, they remove turbulent energy from the maximum energy region and deposit it where the energy is smaller. Both diffusion terms therefore tend to make the turbulence more homogeneous.

A comparison of the turbulence diffusion processes with the spectral transfer processes^{1,2} and the directional-transfer processes arising from the pressure-velocity correlations is instructive.¹ The spectral-transfer processes remove energy from wave number (or eddy-size) regions where the energy is large and deposit it in regions of smaller energy. The directional-transfer processes remove energy from large-energy directional components and deposit it in a directional component (or components) where the energy is smaller. The turbulence-diffusion processes, as shown here, remove energy from regions of space where the energy is large and deposit it in regions of smaller energy. The spectral-transfer, directional-transfer, and turbulence-diffusion processes tend, respectively, to make the turbulence more uniform in wave number space and more isotropic and homogeneous in physical space.

Although one might suppose that turbulence diffusion terms would always tend to make the turbulence more homogeneous, that supposition is not supported by all experimental data. For instance, measurements of wall-bounded turbulence⁶ indicate that the pressure diffusion and the kinetic-energy diffusion terms transfer energy in opposite directions, although the net diffusion is from regions of high to regions of lower energy. On the other hand, measurements of turbulence in a free jet⁷ (closer to the case considered here) seem to support the present findings.

References

1. R. G. Deissler, Phys. Fluids (submitted).
2. R. G. Deissler, Phys. Fluids 24, 1595 (1981).
3. R. A. Clark, J. H. Ferziger, and W. C. Reynolds, J. Fluid Mech. 91, 1 (1979).
4. R. G. Deissler, Phys. Fluids 24, 1911 (1981).
5. P.F. Brinich, D.R. Boldman, and M.E. Goldstein, NASA TN D-8034. 1975.
6. J. Laufer, NACA TR-1174, 1954.
7. I. Wagnanski and H. Fiedler, J. Fluid Mech. 38, 577 (1969).

ORIGINAL PAGE IS
OF POOR QUALITY

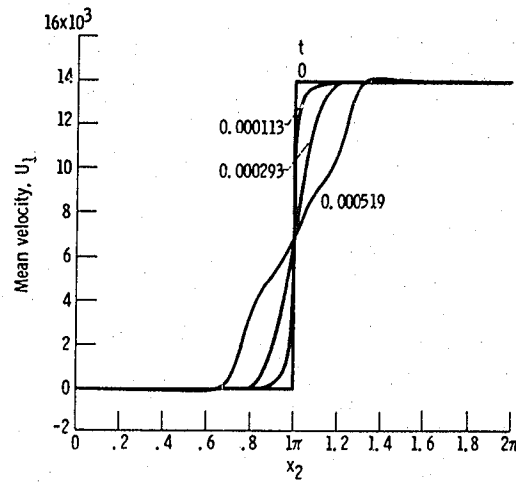


Figure 1. - Calculated development of shear layer mean-velocity profile with dimensionless time, $\frac{u_0^2}{V} t^{1/2}$
 $x_0/V = 554$, $V = 2216$ in Eq. (1).

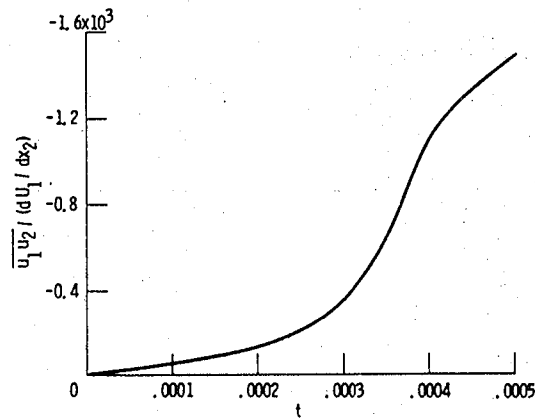


Figure 2. - Calculated time variation of ratio of turbulent to viscous shear stress at $x_2 = \pi$, $\frac{u_0^2}{V} t^{1/2}$, $x_0/V = 554$,
 $V = 2216$ in Eq. (1).

ORIGINAL PAGE IS
OF POOR QUALITY

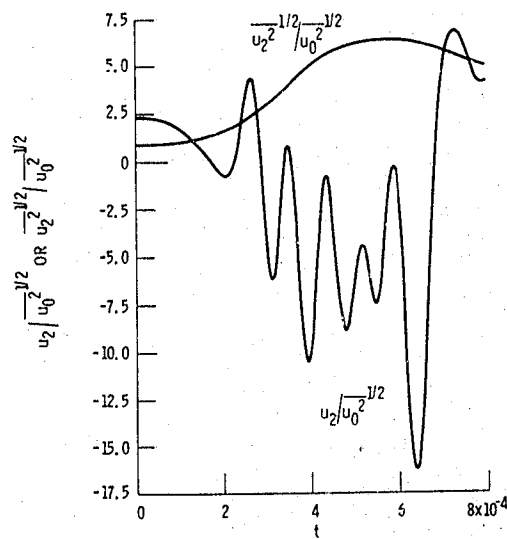


Figure 3. - Calculated evolution of turbulent velocity fluctuations (normalized by initial condition). Un-averaged fluctuations are calculated at center of numerical grid ($x_1 = \pi$). Root-mean-square fluctuations are averaged over x_1 and x_3 at central plane $x_2 = \pi$. $u_0^2 = 554$, $V = 2216$ in Eq. (1).

ORIGINAL PAGE IS
OF POOR QUALITY

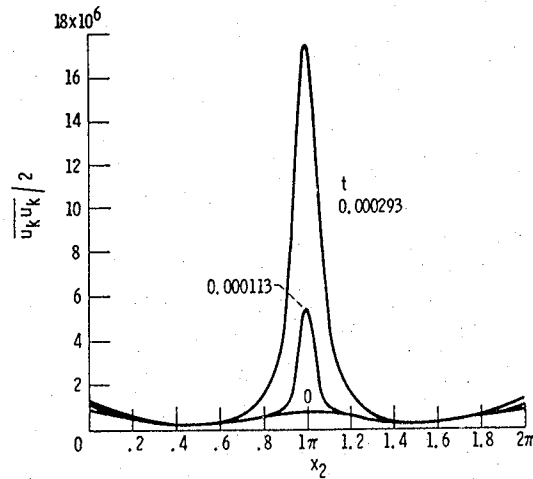


Figure 4. - Development of dimensionless kinetic-energy profile with time. $\frac{u_0^2}{2} x_0/\nu = 554, V = 2216$ in Eq. (1).

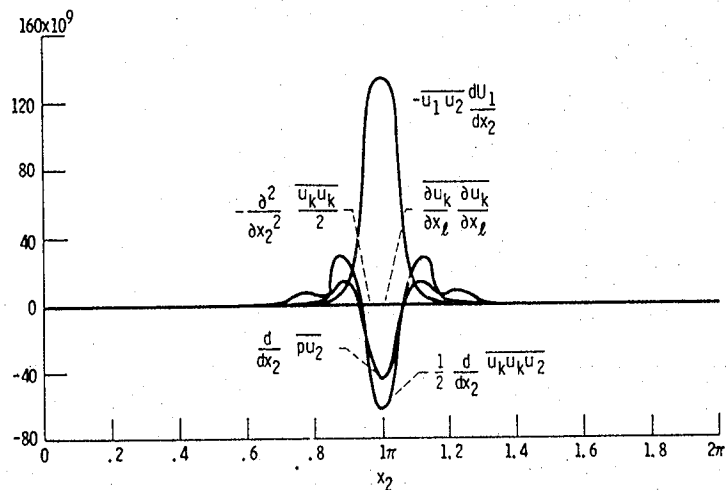


Figure 5. - Plot of terms in one-point correlation equation for kinetic energy $\frac{u_0^2}{2} x_0/\nu = 554, V = 2216$ in Eq. (1), $t = 0.000293$.

End of Document